Stabilizing intrinsic defects in SnO₂

Gul Rahman[*] and Naseem Ud Din

Department of Physics, Quaid-i-Azam University, Islamabad 45320, Pakistan

Víctor M. García-Suárez

Departamento de Física, Universidad de Oviedo, 33007 Oviedo, Spain,
Nanomaterials and Nanotechnology Research Center (CINN), Spain, and
Department of Physics, Lancaster University, Lancaster LA1 4YW, United Kingdom

Erjun Kan

Key Laboratory of Soft Chemistry and Functional Materials (Ministry of Education), and Department of Applied Physics,
Nanjing University of Science and Technology, Nanjing, Jiangsu 210094, P. R. China

The magnetism and electronic structure of Li-doped SnO₂ are investigated using first-principles LDA/LDA+U calculations. We find that Li induces magnetism in SnO₂ when doped at the Sn site but becomes nonmagnetic when doped at the O and interstitial sites. The calculated formation energies show that Li prefers the Sn site as compared with the O site, in agreement with previous experimental works. The interaction of Li with native defects (Sn V_{Sn} and O V_{O} vacancies) is also studied, and we find that Li not only behaves as a spin polarizer, but also a vacancy stabilizer, i.e., Li significantly reduces the defect formation energies of the native defects and helps the stabilization of magnetic oxygen vacancies. The electronic densities of states reveals that these systems, where the Fermi level touches the conduction (valence) band, are nonmagnetic (magnetic).

I. INTRODUCTION

Diluted magnetic semiconductors (DMS) have recently been a major focus of magnetic semiconductor research. In the recent past, ferromagnetism (FM) above room temperature has been extensively investigated in transition metal (TM)-doped wide band gap oxide semiconductors, e.g., ZnO[1,2] and TiO₂.[3–5] Among these wide band gap semiconductors SnO₂ has long been a material of interest for applied and pure research purposes. In 2002, Ogale *et al.*[6] not only reported room temperature FM in Co-doped SnO₂, but also very large magnetic moments. Later on, density functional theory (DFT) calculations showed that Sn vacancies V_{Sn} can induce magnetism in SnO₂ and the observed large magnetic moment was attributed to its influence.[7] Recently, several experimental and theoretical reports showed that cation vacancies can induce magnetism not only in SnO₂, but also in ZnO, TiO₂, ZrO₂, In₂O₃, CeO₂, and HfO₂.[8–13]

Following the prediction of magnetism without TM impurities, much interest was also diverted to magnetism induced by light element doping in host semiconductor matrices, e.g., K, N, Mg, and C-doped SnO₂.[14–18] There are experimental evidences which clearly demonstrate room temperature FM induced by light elements.[19,20] However, the exact nature of magnetism in these semiconductor oxides is still under debate. Recent experimental reports claim that pristine SnO₂ nanocrystalline thin films exhibit room temperature FM, but the magnetic moment is suppressed when doped with Gd.[21] The presence of large amounts of singly ionized oxygen vacancies (V_{O}^{+}), rather than V_{Sn} or V_{O} were found to be responsible for the observed FM in pristine SnO₂ thin films.[21] On the other hand, Chang *et al.*[22] observed FM in very thin pristine SnO₂ films, which was induced by the presence of oxygen vacancies located near the film surface. There is

also a belief that the observed FM in undoped SnO₂ mainly originates from bulk double oxygen vacancies.[23] In contrast, Wang *et al.*[24] studied nanosheets of SnO₂ and they found that the saturation magnetization of all their annealed samples did not feature monodependence on oxygen vacancies, whereas an Sn vacancy related origin was accounted for variations in the magnetization of their studied samples.

Light elements can induce magnetism, but the observed magnetism has also a linkage with native defects. However, whether magnetism is induced by cation or anion vacancies in the pristine host material or doped with light elements, the defect formation energies of native defects, which are important for magnetism, are very high. Oxygen vacancies have lower formation energies,[25] but neutral V_{O} does not induce magnetism in oxides.[7,20,26] The major issue in magnetism induced by vacancies is therefore that these magnetic systems have high formation energies.[27,28] Consequently, to realize defects-driven magnetism experimentally it is essential to reduce the defect formation energy of the host material (SnO₂ in our case). We choose Li as a dopant[29] that can modify the defect formation energies of native defects in SnO₂. We show that Li can indeed significantly reduce the formation energies of various types of defects. This is, as far as we know, the first theoretical study performed on the interaction of Li with native defects in SnO₂.

II. COMPUTATIONAL MODELS AND METHOD

SnO₂ is known to crystallize in the rutile structure with space group $P4_2/mnm$ or D_{14}^{4h} (SG136) under ambient conditions.[30] We used our previously optimized lattice parameters.[7] To simulate the defects a $2 \times 2 \times 2$ supercell of SnO₂ containing 48 atoms was employed. We considered the
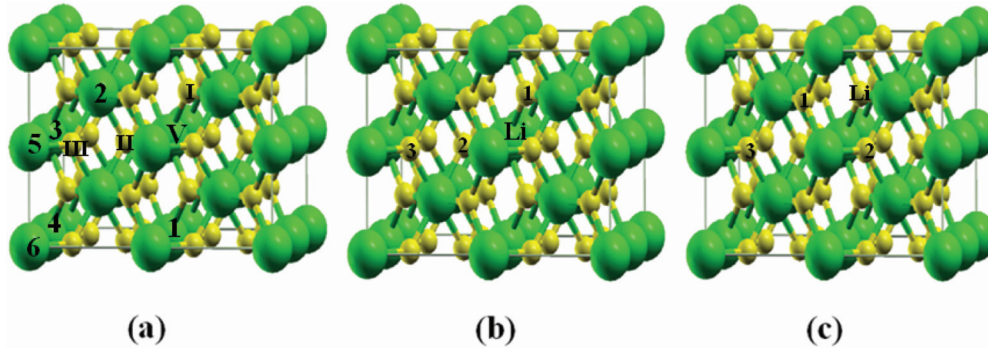
FIG. 1. (Color online) A $2 \times 2 \times 2$ supercell of SnO_2. In (a) V represents the Sn vacancy, which is fixed at the center of the supercell. The positions of Li doped at different Sn sites are marked as 1–6, whereas the positions of Li doped at the O sites are represented by I, II, and III. In model (b) the central atom represents the Li atom doped at the Sn site and the O vacancies are marked as 1–4. In model (c) Li is doped at the O site, marked as Li, and the oxygen vacancies are created at the oxygen sites marked as 1, 2, and 3. Big (green) and small (blue) balls represent Sn and O atoms, respectively.

following models to investigate the detailed energetics and magnetic properties of different defects in SnO_2.

(a) Li-doped SnO_2: Li was doped at the Sn, O, and interstitial sites, denoted as Li_{Sn}, Li_O, and Li_{int}, respectively.

(b) $V_{Sn} + Li_{Snj}$: In this case, V_{Sn} was fixed at the center of the supercell, and Li was doped at different Sn j sites, with $j = 1$–6 [see Fig. 1(a)].

(c) $V_{Sn} + Li_{Oj}$: In this case, V_{Sn} was fixed at the center of the supercell, and Li was doped at different O j sites, with $j = $ I, II, III [see Fig. 1(a)].

(d) $V_{Sn} + Li_{int}$: Here V_{Sn} was fixed at the center of the supercell and Li was doped at interstitial sites.

(e) $V_{Oj} + Li_{Sn}$: Here Li was doped at the central Sn site and V_O was created at different O j sites, with $j = 1$–4 [see Fig. 1(b)].

(f) $V_O + Li_{Oj}$: In this case, V_O was fixed and Li was doped at different O j sites, with $j = 1,2,3$ [see Fig. 1(c)].

(g) $V_O + Li_{int}$: Here V_O was fixed at the center of the supercell and Li was doped at interstitial sites.

We performed calculations in the framework of DFT[31] using linear combination of atomic orbitals (LCAO) as implemented in the SIESTA code.[32] We used a double-ζ polarized (DZP) basis set for all atoms, which included s, p, and d orbitals in Sn and O (we polarized p orbitals, which added an additional five d orbitals) and s and p orbitals in Li (we polarized an s orbital, which added three p orbitals). The local density approximation (LDA)[33] was adopted for describing exchange-correlation interactions. We used standard norm-conserving pseudopotentials[34] in their fully nonlocal form.[35] Atomic positions and lattice parameters were optimized, using a conjugate-gradient algorithm,[36] until the residual Hellmann-Feynman forces converged to less than 0.05 eV/Å. A cutoff energy of 400 Ry for the real-space grid was adopted. This energy cutoff defines the energy of the most energetic plane wave that could be represented on such grid, i.e., the larger the cutoff the smaller the separation between points in the grid ($E \sim G^2 \sim 1/d^2$, where $\bar{G}$ is a reciprocal vector and d is the separation between points). Using the relaxed LDA atomic volume/coordinates, we also carried out LDA+U calculations by considering the on-site Coulomb correction ($U = 6.0$ eV) between the p-orbital electrons of

O.[37,38] We also cross checked some calculations with the VASP code, which uses plane waves and ultrasoft pseudopotentials.[39]

The concentration of dopants and vacancies in a crystal depends upon its formation energies (E_f). The chemical potentials, which vary between the stoichiometric and diluted limits, rely on the material growth conditions and boundary conditions. The chemical potentials of Sn and O depend on whether SnO_2 is grown under O-rich or Sn-rich growth conditions. We have calculated the formation energies under equilibrium conditions, O-rich conditions, and Sn-rich conditions. Under equilibrium conditions, for SnO_2 the chemical potentials of O and Sn satisfy the relationship $\mu_{Sn} + 2\mu_O = \mu_{SnO_2}$, where μ_{SnO_2} is the chemical potential of bulk SnO_2 is a constant value calculated as the total energy per SnO_2 unit formula,[40] and μ_{O_2} is the chemical potential of O which is calculated as total energy per atom of O_2 molecule. The chemical potential of Sn μ_{Sn} is calculated as $\mu_{Sn} = E(Sn^{metal})$, where $= E(Sn^{metal})$ is the total energy per atom of bulk Sn. For equilibrium condition we used $\mu_{Sn} = \mu_{SnO_2} - 2\mu_O$ and $\mu_O = (\frac{\mu_{SnO_2} - \mu_{Sn}}{2})$. Under Sn rich conditions, $\mu_{Sn} = E(Sn^{metal})$, $\mu_O = (\frac{\mu_{SnO_2} - \mu_{Sn}}{2})$. O-rich condition gives $\mu_O = (\frac{1}{2})E(O_2)$, $\mu_{Sn} = \mu_{SnO_2} - 2\mu_O$. Note that μ_{Sn} and μ_O are not independent, but vary between the Sn-rich and O-rich limits under a constraint defined by the equilibrium condition of SnO_2. The Sn-rich limit corresponds to the upper limit of μ_{Sn} and also the lower limit of μ_O. Therefore it is expected that different chemical potential will give different defect formation energies.[41]

The formation energies for systems with intrinsic defects, either Sn or O vacancies, can be calculated in the following way:

$$E_f = E^d - E^p + n\mu_X, \quad (1)$$

where μ_X is chemical potential of X (X = Sn, O), n is the number of atoms removed from the system, and E^d and E^p are the total energies of the defected and the pure system, respectively.

The formation energy of the Li-doped system can be calculated as

$$E_f = \frac{1}{n}(E^d - E^p + n\mu_X - m\mu_{Li}), \quad (2)$$

where μ_{Li} is the chemical potential of bulk lithium, calculated as the total the energy per unit cell of bulk Li, n is number of atoms removed, and m is number of atoms added to the system. We note again that some of these energies, which are very sensible, were cross checked with the VASP code.

III. RESULTS AND DISCUSSIONS

As stated above, we relaxed all the systems, so we will only discuss the relaxed data. Comparisons will be made with the unrelaxed data where necessary. It is important to discuss the implication of the LDA+U approach before starting the discussion of the calculated results. Our LDA calculations show that SnO$_2$ has a band gap of 0.9 eV which is comparable with previous LDA calculations.[42] It is known that LDA underestimates the band gap of materials, which can be corrected by applying the LDA+U approach. The LDA+U calculated band gap of SnO$_2$ in our case is ∼3.10 eV, which is comparable with the experimental and theoretical values of 3.20 eV.[43,44] It is to be noted that the formation energies of relaxed LDA systems can also be affected by the U term, which will be discussed wherever required. For electronic structures (densities of states), we will only show the LDA+U calculated results, because LDA does not reproduce accurately the band gap, as stated above.

First, we will focus on Li-doped SnO$_2$ and then we will move to discuss the interaction of Sn and O vacancies with Li.

A. Li-doped SnO$_2$

First, we calculate, using the above equations, the defect formation energies of the doped SnO$_2$ systems, where Li was doped at the Sn, O, and interstitial sites, as stated before. The calculations (see Table I) show that the doping of Li at the Sn site has the lowest formation energy (−1.03 eV) under stoichiometric and O-rich conditions, as compared with the O site. Although Li at the interstitial site has the lowest formation energy among the three dopant sites, it is not important from the magnetism point of view. For comparison purposes, the formation energies of the LDA+U systems are also given in Table I. Our detailed structural relaxation analysis shows that structural relaxation is not very effective when Li is doped at the Sn site. This behavior can easily be understood in terms of the atomic sizes of the Sn and Li atoms. The atomic radii of Sn and Li are 1.41 and 1.45 Å, respectively. The doped Li is surrounded by six O atoms and the optimized bond lengths

between them (LiO distances) have two different values, 1.97 and 2.03 Å, which are comparable to the pure bond lengths of SnO in SnO$_2$, i.e., 2.04 and 2.08 Å. Due to the radius similarity, Li at the Sn site will not distort the structure and it is therefore expected that the Sn site will be favorable for Li doping. Indeed our calculations also show that Li at the Sn site has the lowest formation energy as compared with the O site, which agrees with experimental observations.[29] On the other hand, we found that the unrelaxed Li at the O site has a large formation energy under the equilibrium condition. The formation energy of Li at the O site was very large when structural relaxation was not allowed but decreased significantly when structural relaxation was permitted, which produced a large structural distortion. The structural analysis showed that when Li is doped at the O site, it goes to an interstitial site and leaves behind an O vacancy. So, this indicates that the formation energy of O is lowered mainly due to a structural deformation which is accompanied by the movement of Li to an interstitial position. At the same time, the system remains nonmagnetic. To be more confident, we also carried out separate calculations on Li at interstitial sites with and without O vacancies, and we got the same conclusion, which will be discussed below. Comparing the LDA and LDA+U calculated formation energies, it is clear that LDA+U changes only the formation energy of the Li$_O$ system, whereas the rest of the cases remain similar.

As stated above, doped Li prefers the Sn site under stoichiometric and O-rich conditions, where it has a large magnetic moment (3.00 μ_B). Since the nominal valence of Sn in a perfect SnO$_2$ is Sn^{4+}, and Li is a cation with valence of Li^{1+},[29] when Li is doped at the Sn site in pure SnO$_2$, it donates one electron to compensate one hole among the four holes generated by the Sn deficiency. The three uncompensated holes, localized at the O sites, give a magnetic moment of 3.00 μ_B per supercell. Table I clearly shows that LDA+U does not change the total magnetic moments of the doped/defected systems, in agreement with previous theoretical calculations which have also shown that the inclusion of the U term does not change the magnetic moments caused by vacancies.[45,46] To see the atomic origin of magnetism in Li-doped SnO$_2$, we calculated the total and atom projected partial density of states (PDOS) of the Sn, O, and Li atoms (see Fig. 2). As can be seen, the substitutional Li impurity polarizes the host band, which gives rise to an induced impurity peak close to the valence band edge in the spin-down part of the total DOS, while the spin-up part is influenced slightly. Such a behavior suggests that Li behaves as a p type dopant in SnO$_2$.[29] The low lying s orbitals of Li are spin polarized and strongly hybridized with the p orbitals of O. The Fermi energy is mainly dominated by the p orbitals of O, which indicates that magnetism is mainly induced by the p orbitals and localized at the O atom. Indeed, the oxygen atoms surrounding the doped Li are the main ones that contribute to magnetism. We also see that the spin-down state is partially occupied which contributes to the magnetic moment. The majority s spin states of Li are completely occupied and the minority spin states are partially occupied, leading to a significant spin splitting near the Fermi level.

To further emphasize the nature of magnetism, the spin density contours are shown in Fig. 3. It is interesting to see that Li polarizes the O and Sn atoms in opposite directions, and the polarization is not only limited to the nearest O atoms
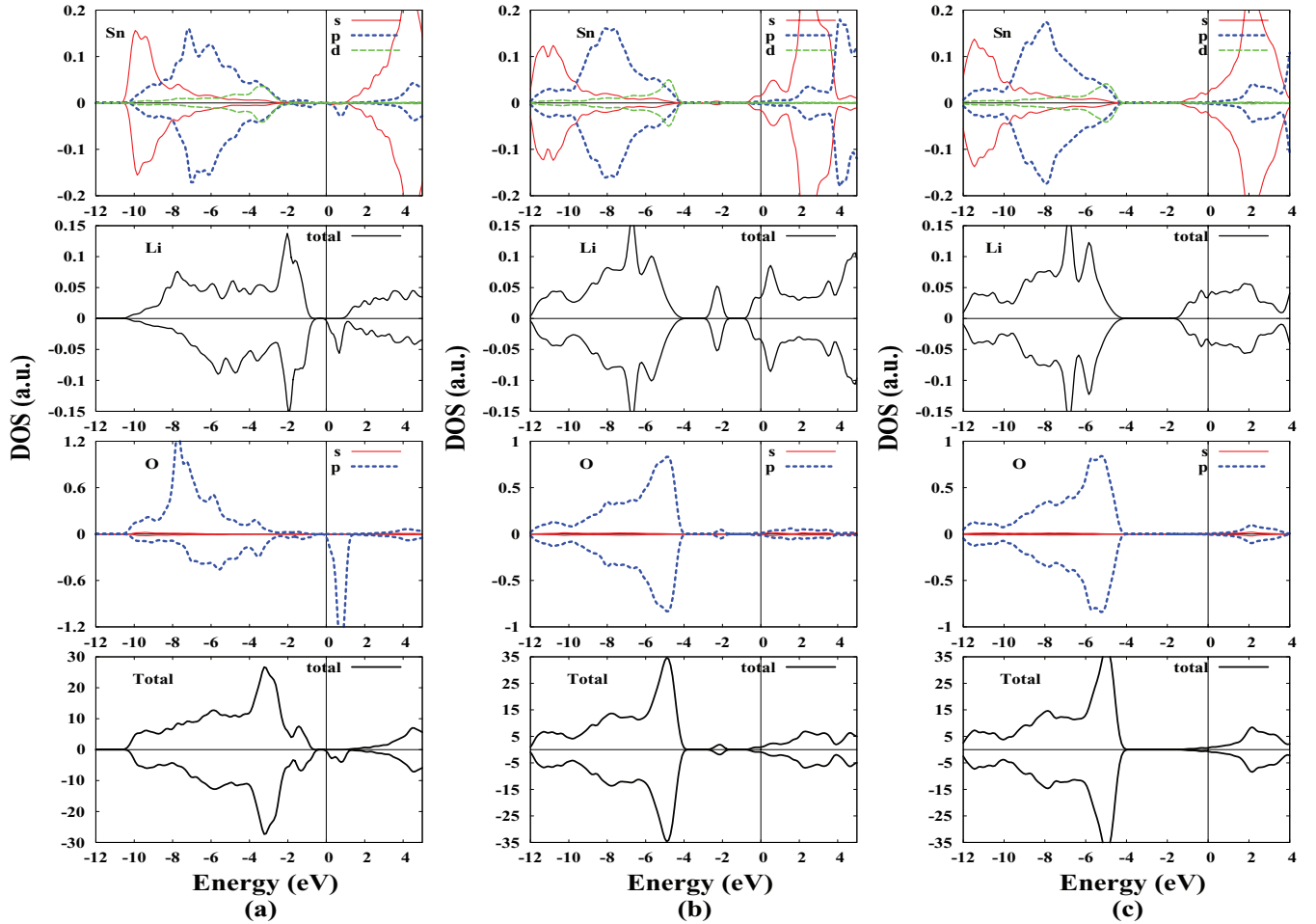
TABLE I. Formation energies calculated under equilibrium (E_{eq}), Sn-rich (E_{Sn}), and O-rich (E_{O}) conditions, in units (eV). The last column lists magnetic moments (MM) per supercell, calculated in units of μ_B. Values in parentheses show formation energies calculated with LDA+U.

System	E_{eq}	E_{Sn}	E_{O}	MM
Li$_{\text{Sn}}$	−1.03(−0.84)	6.53(6.14)	−1.03(−0.84)	3.00(3.00)
Li$_{\text{O}}$	−0.85(1.83)	−0.85(1.83)	2.93(5.32)	0.00(0.00)
Li$_{\text{int}}$	−2.58(−2.05)	−2.58(−2.05)	−2.58(−2.05)	0.00(0.00)
V$_{\text{Sn}}$	6.87(8.64)	14.44(15.62)	6.87(8.64)	4.00(4.00)
V$_{\text{O}}$	1.64(4.40)	1.64(4.40)	5.42(7.89)	0.00(0.00)

FIG. 2. (Color online) The LDA+U calculated total and partial density of states (DOS) of (a) Li$_{Sn}$, (b) Li$_O$, and (c) Li$_{int}$ systems. Solid (red) and dashed (blue, green) lines represent s and p, d states, respectively. In the bottom panels the solid line represents the total DOS. The positive (negative) DOS shows majority (minority) spin states. The Fermi level (E_F) is set to zero.

surrounding the Li atoms, but it also spreads to other O atoms which are far from the Li. It seems that the origin of magnetism in light elements doped-SnO$_2$ or Sn vacancies in SnO$_2$ is the same, i.e., the polarization of the surrounding O atoms. However, the remarkable feature of Li doped SnO$_2$ is that there is a very small (negligible) induced magnetic moment at the Li

FIG. 3. (Color online) Spin density contours for the Li-doped SnO$_2$ (110) plane. Labels show atomic sites.

site. This behavior is quite different from other light elements doped SnO$_2$ systems,[14–16] which suggests that Li behaves as a spin polarizer in SnO$_2$. We note that Li doped at the O and interstitial sites does not induce magnetism (see Fig. 2). Test calculations on a supercell of $2 \times 2 \times 3$ (containing 72 atoms) were also carried out and we found the same behavior, i.e., Li at the Sn site gives 3.00 μ_B magnetic moment per supercell, whereas Li at the O site does not show any magnetic moment. Using a larger supercell does change the defect formation energy of the defected systems.[47,48] Additional calculations were also carried out to see the magnetic coupling between the Li atoms since it is known that the magnetic coupling between the impurity atoms depend on the separation between the defects/impurities.[7,49] The results show that Li couples ferromagnetically.[50]
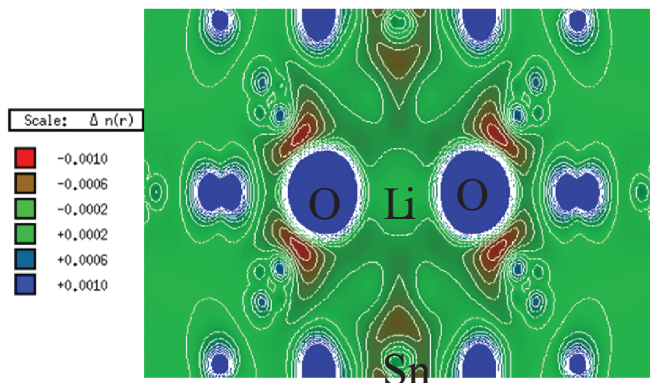
B. Interaction of Sn vacancies with Li

We will move now to discuss the interaction of intrinsic defects (Sn and O vacancies) with Li. We found that a single Sn vacancy induces a very large magnetic moment (LDA and LDA+U) ~ 4.00 μ_B, which agrees with previous calculations.[7] However, V$_{Sn}$ has a very large formation energy

TABLE II. Formation energies (in units of eV) of systems $V_{Sn} + Li_{Sn}$, $V_{Sn} + Li_{O}$, and $V_{Sn} + Li_{int}$ calculated under equilibrium (E_{eq}), Sn-rich (E_{Sn}), and O-rich (E_{O}) conditions. The distance from V_{Sn} to Li_{Sn}, Li_{O}, and Li_{int} is $r - r_j$ (in units of Å). The last column lists the calculated magnetic moments (MM) per supercell (in units of μ_B). Values in parentheses show formation energies calculated with LDA+U.

System	$r - r_j$	E_{eq}	E_{Sn}	E_{O}	MM
$V_{Sn} + Li_{Sn_j}$					
$V_{Sn} + Li_{Sn1}$	3.23	1.55(1.77)	9.11(8.75)	1.55(1.77)	7.00(7.00)
$V_{Sn} + Li_{Sn2}$	3.76	2.13(2.64)	9.69(9.62)	2.13(2.64)	7.00(7.00)
$V_{Sn} + Li_{Sn3}$	4.80	1.54(2.45)	9.10(9.43)	1.54(2.45)	7.00(7.00)
$V_{Sn} + Li_{Sn4}$	5.78	1.56(2.42)	9.13(9.40)	1.56(2.42)	7.00(7.00)
$V_{Sn} + Li_{Sn5}$	6.79	2.80(2.65)	10.36(9.63)	2.80(2.65)	7.00(7.00)
$V_{Sn} + Li_{Sn6}$	7.52	2.91(2.80)	10.48(9.78)	2.91(2.80)	7.00(7.00)
$V_{Sn} + Li_{O_j}$					
$V_{Sn} + Li_{OI}$	2.04	−4.16(−2.58)	3.40(4.40)	−0.38(0.91)	1.00(1.00)
$V_{Sn} + Li_{OII}$	2.08	−1.74(−1.84)	3.82(5.14)	0.04(1.65)	1.00(1.00)
$V_{Sn} + Li_{OIII}$	4.71	6.09(12.56)	13.65(19.54)	4.93(16.05)	1.00(1.00)
$V_{Sn} + Li_{int}$					
$V_{Sn} + Li_{int}$	5.73	1.83(2.35)	9.40(9.32)	1.83(2.35)	3.00(3.00)

in both O-rich (6.87 eV) and Sn-rich(14.44 eV) conditions, which is not significantly reduced after structural relaxation. To decrease the formation energy of V_{Sn}, which is the core of this article, we doped Li at different Sn sites (see Fig. 1), with the Sn vacancy at the center of the supercell. The formation energies are given in Table II. As can be seen, by doping Li at the Sn site, the defect formation energy of V_{Sn} is significantly reduced. The case $V_{Sn} + Li_{Sn3}$ has the lowest formation energy $\sim$1.54 eV, which shows that Li doping is much more favorable energetically in SnO$_2$ than previously reported Zn[27] and Cr[28] doping: The formation energies of the system with $Zn_{Sn} + V_{Sn}$ are 16.50 and 7.00 eV under O-poor and the O-rich conditions,[27] respectively. Doping Cr in SnO$_2$ with V_{Sn} produces formation energies $\sim$12.00 and 2.00 eV under O-poor and O-rich conditions,[28] respectively. All these previous calculations were carried out without U. In our case the formation energies are 9.10 and 1.54 eV under O-poor and O-rich conditions, respectively. It is interesting to see that Li not only stabilizes V_{Sn}, but also produces the largest magnetic moment, 7.00 μ_B, per supercell. The origin of such magnetic moment is due to the three uncompensated holes of Li at the Sn site along with the four holes of neutral V_{Sn}.

Once we found that Li at Sn sites significantly reduces the defect formation energy of Sn vacancies, we doped Li at the O site in the presence of V_{Sn}. In this case, we also fixed V_{Sn} and doped Li at different O sites, mainly considering those O atoms which are near and far from V_{Sn}. The calculated formation energies are shown in Table II. We can see that the unrelaxed systems have large positive formation energies (endothermic processes), but after structural relaxation they turn to negative formation energies (exothermic processes). This effect of structural relaxation on the defect formation energies was also confirmed using VASP. For example, the relaxed (unrelaxed) defect formation energy of the $V_{Sn} + Li_{O_{II}}$ system under equilibrium conditions was found to be −3.74 (5.39) eV using the SIESTA code, whereas VASP gave −4.08 (4.51) eV. When Li was doped at O sites around V_{Sn} it moves to an interstitial configuration (near V_{Sn}) after structural relaxation. This exothermic process leaves behind an oxygen vacancy and an interstitial Li near V_{Sn} (see Fig. 4), which indicates

that doped Li does not prefer the O site, but the interstitial site. As shown also above, the Li_O and Li_{int} systems have no magnetic moment, whereas V_{Sn} has a large magnetic moment. However, when Li is doped at the O site, three out of the four holes generated by V_{Sn} are compensated by the 2$^-$ charge state of V_O and one electron of Li, leaving behind a single hole that gives a magnetic moment of 1.00 μ_B. When Li is far from V_{Sn} ($V_{Sn} + Li_{OIII}$ case), it does not form a stable structure.

We discuss now the interaction of Sn vacancies with Li_{int}. In this case, we doped Li at an interstitial site which was 5.37 Å away from V_{Sn}. The defect formation energy of this system is given in Table II. Although the $Li_{int} + V_{Sn}$ system behaves endothermically, the formation energy of V_{Sn} decreases a lot as compared with the V_{Sn} system without Li_{int}. Note that the structural relaxation does not change the sign of E_f. The $Li_{int} + V_{Sn}$ system also shows a magnetic moment, 3.00 μ_B per supercell. In other words, when Li is at the interstitial site it interacts with V_{Sn} and reduces its magnetic moment.
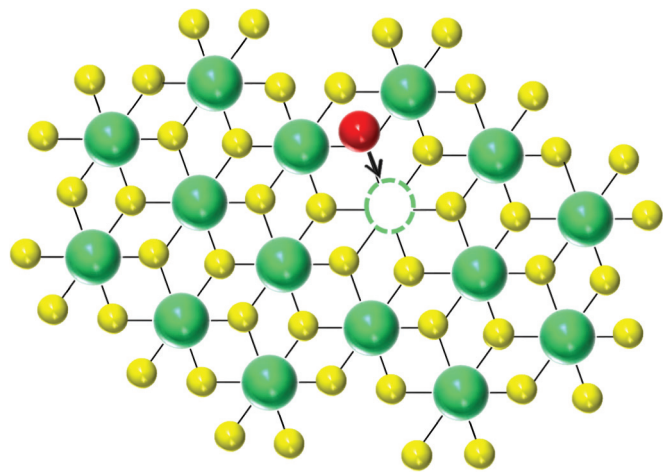

FIG. 4. (Color online) Schematic representation of the structural relaxation in the $Li_O + V_{Sn}$ system. Green, yellow, and red balls represent Sn, O, and Li atoms, respectively. The Sn vacancy (V_{Sn}) is represented by a green dashed circle. The arrow represents the movement of the Li atom towards V_{Sn} during the structural relaxation.

From the thermodynamics of different defects in SnO_2, we can conclude that among all these defects the $V_{Sn} + Li_O$ complex has the lowest energy. In the presence of vacancies (Sn and O), Li prefers to occupy the O site rather than going into Sn or interstitial sites. Although interstitial Li also reduces the formation energy of V_{Sn}, it is not a favorable process. Note that different defective systems of Li-doped ZnO showed the same type of behavior in a previously reported work.[20]

It is very interesting that irrespective of the location of Li in Sn defective systems, it always reduces the formation energy of V_{Sn} and the systems remains magnetic both with LDA and LDA+U. To further understand the electronic structure of doped SnO_2 and the interaction of Li with native defects, we show the LDA+U calculated total and atom projected densities of states in Fig. 5. The interaction of Li with native defects mainly affects the local DOS of the O atoms. Also, Li-O hybridizations can be seen around the Fermi levels. In all LDA cases, the oxygen spin-up p orbitals were occupied, whereas the spin-down p orbitals were partially occupied, similar to the DOS of V_{Sn}.[7] With LDA+U the oxygen p orbitals are almost totally occupied, as expected due to the U.

C. Interaction of O vacancies with Li

It is believed that Sn vacancies have higher formation energy as compared with O vacancies. Indeed, we found that the O vacancy has a defect formation energy (1.64 eV) much smaller than that for the Sn vacancy. We therefore considered also the interactions of O vacancies with Li. First, we doped Li at the Sn site and varied the position of the O vacancy. The calculated defect formation energies are shown in Table III. Interestingly, doping of Li at the Sn site appreciably reduced the defect formation energy of V_O. The defect complex $V_{O3} + Li_{Sn}$ has the lowest formation energy, −3.69 eV, in equilibrium conditions. Note that our VASP calculations show −3.90 eV for the same defect complex. Such a favorable process implies that oxygen vacancies also promote magnetism in doped systems. We must stress that oxygen vacancies by themselves are nonmagnetic,[7] but however, become magnetic in the presence of Li_{Sn}, which is also magnetic. Either Li_{Sn} or V_O have large defect formation energies, but the defect complex $V_O + Li_{Sn}$ has a lower energy than the individual defects. It

is interesting to see that these defect complexes always give magnetism with magnetic moments of 1.00 μ_B, no matter how far V_O is from Li_{Sn}. Such behavior is different from Co-doped SnO_2, where it has been shown that V_O quenches magnetism when Co_{Sn} is away from V_O.[51] On the other hand, Ni-doped SnO_2 does not show magnetism without V_O.[52] We therefore believe that Li-doped SnO_2 is another candidate material for spintronics. We also found that V_O and Li_O do not induce magnetism in SnO_2, as seen in Table III, but the formation energy of this complex is always bigger than that of the $V_O + Li_{Sn}$ complex, excluding under Sn-rich conditions. There are some experimental reports which claim that oxygen vacancies are responsible for room temperature ferromagnetism in oxides,[53] but to date none of them show that a single neutral V_O is the main source of magnetism in SnO_2. Generally, it is believed that V_O promotes magnetism in doped SnO_2,[51,52] which is proven by our extensive calculations (see Table III). We also considered Li at different O sites in the presence of O vacancies but the calculated E_f show that these configurations are less stable than the $V_O + Li_{Sn}$ (excluding Sn-rich conditions).

The interaction of O vacancies with Li_{int} was also taken into account. The calculated E_f of $Li_{int} + V_O$ are given in Table III which shows that the behavior of $Li_{int} + V_O$ is quite different from $Li_{int} + V_{Sn}$. Li_{int} reduces the formation energy of V_{Sn}, but however Li_{int} does not decrease the formation energy of V_O. Also such kinds of defect complexes have zero magnetic moments. Both LDA and LDA+U calculations give the same magnetic moments, as found before. From Tables II and III we can therefore see that E_f can be reduced by Li. On one hand, in the presence of a Sn vacancy, the probable location of Li will be the O site, where structural relaxation is also expected. On the other hand, Li prefers the Sn site rather than the O site, when the interactions of O vacancies with Li_O is considered.

Before summarizing our work, the electronic structure of the above mentioned defect complexes will be presented. Figure 6(a) shows that the LDA+U electronic structure is similar to Li_{Sn}, i.e., the magnetism is mainly contributed by the O p orbitals and the Li-O type hybridization can also be seen near the Fermi level. Oxygen or tin vacancies localize the oxygen p orbitals of the other O atoms in the presence of Li_{Sn} [see Figs. 5(a) and 6(a)]. No magnetism

TABLE III. Formation energies (in units of eV) of systems $V_O + Li_{Sn}$, $V_O + Li_O$, and $V_O + Li_{int}$ calculated under equilibrium (E_{eq}), Sn-rich (E_{Sn}), and O-rich (E_O) conditions. The distance from V_O to Li_{Sn}, Li_O, and Li_{int} is $r - r_j$ (in units of Å). The last column lists the calculated magnetic moments (MM) per supercell (in units of μ_B). Values in parentheses show formation energies calculated with LDA+U.

| System	$r - r_j$	E_{eq}	E_{Sn}	E_O	MM
$V_{Oj} + Li_{Sn}$					
$V_{O1} + Li_{Sn}$	2.04	−2.55(−1.88)	5.01(5.10)	1.23(1.61)	1.00(1.00)
$V_{O2} + Li_{Sn}$	2.08	−2.34(−2.76)	5.22(4.22)	1.44(0.73)	1.00(1.00)
$V_{O3} + Li_{Sn}$	4.71	−3.69(−0.02)	3.87(6.96)	0.09(3.47)	1.00(1.00)
$V_{O4} + Li_{Sn}$	5.71	−2.09(0.05)	3.39(7.02)	−0.39(3.54)	1.00(1.00)
$V_O + Li_{Oj}$					
$V_O + Li_{O1}$	2.94	0.15(2.57)	0.15(2.57)	3.93(6.06)	0.00(0.00)
$V_O + Li_{O2}$	3.47	0.21(2.71)	0.21(2.71)	3.98(6.20)	0.00(0.00)
$V_O + Li_{O3}$	5.15	0.30(3.06)	0.30(3.06)	4.08(6.55)	0.00(0.00)
$V_O + Li_{int}$					
$V_O + Li_{int}$	3.48	−0.96(1.63)	−0.96(1.63)	1.36(5.11)	0.00(0.00)
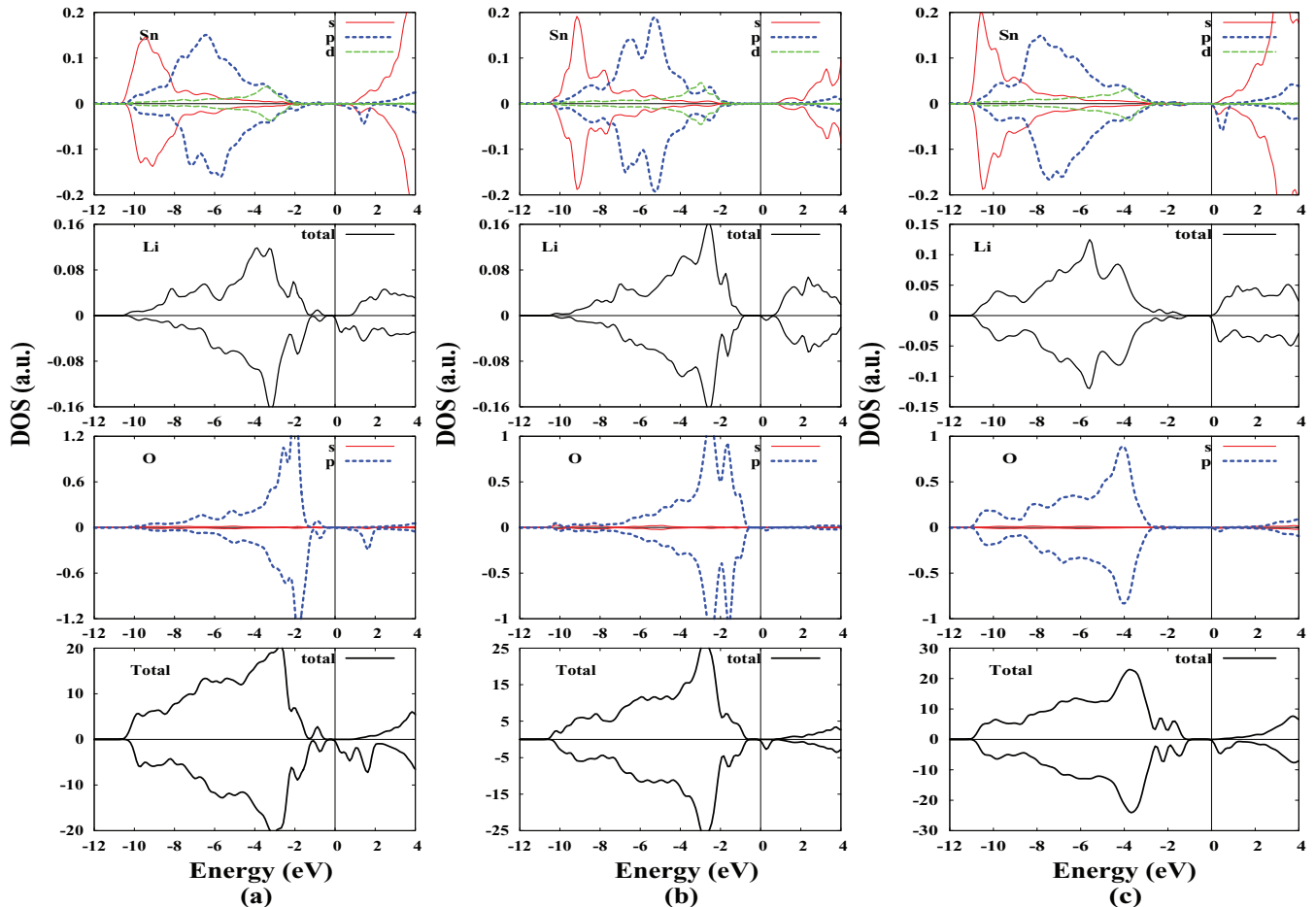
FIG. 5. (Color online) The LDA+U calculated total and partial density of states (DOS) of (a) V$_{Sn}$ + Li$_{Sn}$, (b) V$_{Sn}$ + Li$_O$, and (c) V$_{Sn}$ + Li$_{int}$ systems. Solid (red) and dashed (blue, green) lines represent s, p and d states, respectively. The bottom panel solid line represents the total DOS. The positive (negative) DOS shows majority (minority) spin states. The Fermi level (E_F) is set to zero.

can be seen in Fig. 6(b), which represents the V$_O$ + Li$_O$ defect system. The impurity peak around 2 eV below E_F is contributed by the Li atom. The conduction and valance bands are separated from each other and the Fermi level crosses the conduction band, which is mainly formed by Sn s and Li orbitals. This electronic structure indicates that Li in the V$_O$ system will behave as an electron donor. The electronic structure of V$_O$ + Li$_{int}$ [Fig. 6(c)] also shows nonmagnetic behavior. The O p orbitals are completely occupied and are far from E_F. The Li and Sn atoms occupy the conduction band, which is also crossed by the Fermi level, i.e., V$_O$ + Li$_{int}$ is also a n-type material. Comparing the DOS of the Li$_{int}$ system with that of the V$_O$ + Li$_{int}$, we see that V$_O$ pushes the valence band of Li$_{int}$ to lower energies. From the given DOS in Figs. 2, 5, and 6, we may say that those systems in which E_F cuts the conduction bands, i.e., which behave as electron donors, do not show magnetism. This indicates that magnetism in SnO$_2$ is mediated by holes and destroyed by electrons. Further experimental work is needed to validate these theoretical predictions.

We have shown that the band gap of SnO$_2$ can easily be recovered using the LDA+U approach. It is also interesting to note that the defect formation energies of defective systems can be improved by LDA+U, according to calculations on binding

energies of similar defective systems.[54–56] However, recent progress in DFT shows that defect states can be more accurately described with hybrid functionals, such as the (atomic) self-interaction corrected functional (SIC or ASIC) or the Heyd, Scuseria, and Ernzerhof (HSE) functional.[56–62] These approaches can accurately account for the self-interaction correction, which not only act upon the levels on which U is applied but on the whole electronic structure. Hence, more accurate defect states are expected from such types of calculations. However, this does not change the main conclusion of our work, as similarly pointed out by Janotti *et al.*,[56] who compared the defect formation energies of ZnO using LDA+U and hybrid approaches. Carter *et al.*[59] also studied defects in GaN using GGA and SIC, and both approaches gave qualitatively the same results. A recent comparative study between the LDA+U and the HSE hybrid functional in ZnO shows that the defects thermodynamics can correctly be described by LDA+U.[57] Therefore, although it is expected that SIC (or ASIC) and HSE would have more profound effects on the electronic structure, we believe that LDA+U can correctly describe defects in SnO$_2$, at least qualitatively.

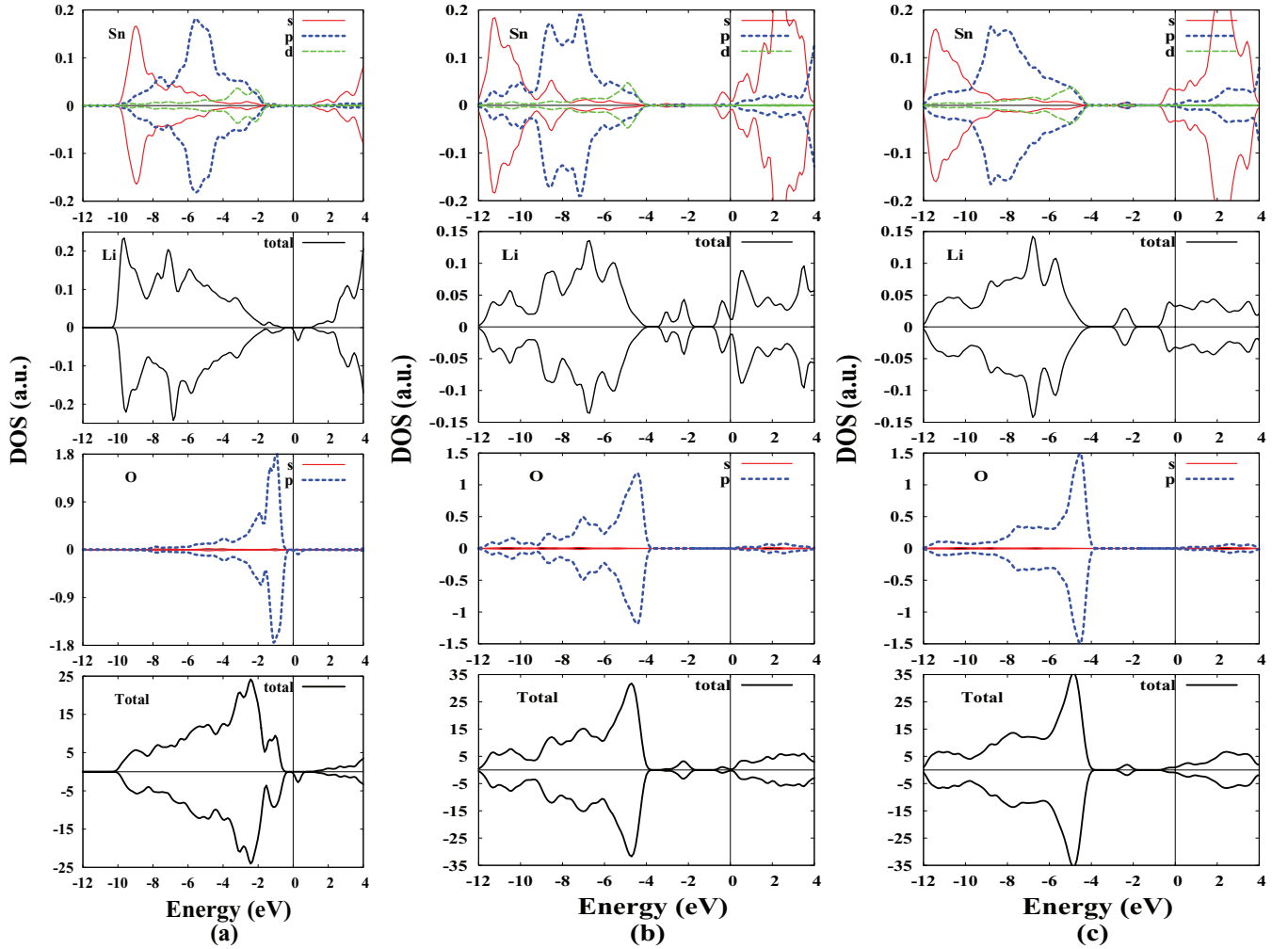A note of caution should be added however when comparing the formation energies of oxygen defects with those of other

FIG. 6. (Color online) The LDA+U calculated total and partial density of states (DOS) of (a) V_O + Li_{Sn}, (b) V_O + Li_O, and (c) V_O + Li_{int} systems. Solid (red) and dashed (blue, green) lines represent s, p and d states, respectively. The bottom panel solid line represents the total DOS. The positive (negative) DOS shows majority (minority) spin states. The Fermi level (E_F) is set to zero.

defects, since the application of the U functional on the oxygen p states particularly improves the electronic structure of oxygen related defects, as opposed to a bare-LDA less accurate treatment of other cases. However, the relative trends with/without U are the same for all cases and the differences induced by the U on the oxygen defects are comparable to the rest of defects (although larger, see Table I). For these reasons we believe these results are qualitatively correct. Notice again that a more general treatment with hybrid functionals such as SIC[59,61] or HSE[58] would affect more democratically the whole electronic structure and improve the results.

IV. SUMMARY

We investigated the energetics and magnetism of Li-doped SnO_2 systems with and without native defects using density functional theory (DFT) with LDA and LDA+U. Lithium was doped at Sn, O, and interstitial sites and it was shown that it can induce magnetism in SnO_2 when doped at the Sn site. No magnetism was found however when Li was doped at the O and interstitial sites. The defect formation energies showed that Li doped at the Sn site is more favorable than doped at the O site.

We found that Li at the Sn site also shows a large magnetic moment (3.00 μ_B), and the origin of magnetism was discussed in terms of electronic structures and spin densities. Native defects, Sn vacancies (V_{Sn}) and O vacancies (V_O), were also studied and it was observed that magnetic V_{Sn} has higher defect formation energy than nonmagnetic V_O. To reduce the defect formation energies of these native defects, the interactions of Li with V_{Sn} and V_O were also studied. The calculated defect formation energies of these native defects were significantly decreased by Li. Our calculations showed that V_O helps to promote magnetism in Li-doped SnO_2, in agreement with general experimental speculations. Structural relaxations were shown to be important when the interactions of Li with V_{Sn} were considered. Comparison of our studied system with previously synthesized systems was also discussed and it was concluded that Li-doped SnO_2 is another good candidate in the filed of spintronics.

---

*gulrahman@qau.edu.pk

[1] K. Ueda, H. Tabata, and T. Kawai, Appl. Phys. Lett. **79**, 988 (2001).

[2] K. Yang, R. Wu, L. Shen, Y. P. Feng, Y. Dai, and B. Huang, Phys. Rev. B **81**, 125211 (2010).

[3] K. S. Yang, Y. Dai, and B. B. Huang, J. Chem. Phys. **10**, 2327 (2009).

[4] K. S. Yang, Y. Dai, B. B. Huang, and M. H. Whangbo, Appl. Phys. Lett. **93**, 132507 (2008).

[5] K. S. Yang, Y. Dai, B. B. Huang, and Y. P. Feng, Phys. Rev. B **81**, 033202 (2010).

[6] S. B. Ogale, R. J. Choudhary, J. P. Buban, S. E. Lofland, S. R. Shinde, S. N. Kale, V. N. Kulkarni, J. Higgins, C. Lanci, J. R. Simpson, N. D. Browning, S. Das Sarma, H. D. Drew, R. L. Greene, and T. Venkatesan, Phys. Rev. Lett. **91**, 077205 (2003).

[7] G. Rahman, V. M. García-Suárez, and S. C. Hong, Phys. Rev. B **78**, 184404 (2008).

[8] M. Khalid, M. Ziese, A. Setzer, P. Esquinazi, M. Lorenz, H. Hochmuth, M. Grundmann, D. Spemann, T. Butz, G. Brauer, W. Anwand, G. Fischer, W. A. Adeagbo, W. Hergert, and A. Ernst, Phy. Rev. B **80**, 035331 (2009).

[9] D. Kim, J. Hong, Y. Ran Park and K. Joo Kim, J. Phys.: Condens. Matter **21**, 195405 (2009).

[10] F. Máca, J. Kudrnovský, V. Drchal, and G. Bouzerar, Appl. Phys. Lett. **92**, 212503 (2008).

[11] L. X. Guan, J. G. Tao, C. H. A. Huan, J. L. Kuo, and L. Wang, J. Appl. Phys. **108**, 093911 (2010).

[12] V. Fernandes, P. Schio, A. J. A. de Oliveira, W. A. Ortiz, P. Fichtner, L. Amaral, I. L. Graff, J. Varalda, N. Mattoso, W. H. Schreiner, and D. H. Mosca, J. Phys.: Condens. Matter **22**, 216004 (2010).

[13] J. Osorio-Guillén, S. Lany, S. V. Barabash, and A. Zunger, Phy. Rev. B **75**, 184421 (2007).

[14] S. K. Srivastava, P. Lejay, B. Barbara, S. Pailhés, V. Madigou, and G. Bouzerar, Phys. Rev. B **82**, 193203 (2010).

[15] W. Zhi Xiao, L. Ling Wang, L. Xu, Q. Wan, and Zou, Solid State Commun. **149**, 1304 (2009).

[16] C. Wen Zhang, and S. shen Yan, Appl. Phys. Lett. **95**, 232108 (2009).

[17] G. Rahman and V. M. García-Suárez, Appl. Phys. Lett. **96**, 052508 (2010).

[18] N. H. Hong, J. H. Song, A. T. Raghavender, T. Asaeda, and M. Kurisu, Appl. Phys. Lett. **99**, 052505 (2011).

[19] N. Hoa Hong, J. H. Song, A. T. Raghavender, T. Asaeda, and M. Kurisu, Appl. Phys. Lett **99**, 052505 (2011).

[20] J. B. Yi, C. C. Lim, G. Z. Xing, H. M. Fan, L. H. Van, S. L. Huang, K. S. Yang, X. L. Huang, X. B. Qin, B. Y. Wang, T. Wu, L. Wang, H. T. Zhang, X. Y. Gao, T. Liu, A. T. S. Wee, Y. P. Feng, and J. Ding, Phys. Rev. Lett. **104**, 137201 (2010).

[21] S. Ghosh, G. G. Khan, and K. Mandal, Appl. Mater. Interfaces. **4**, 2048 (2012).

[22] G. S. Chang, J. Forrest, E. Z. Kurmaev, A. N. Morozovska, M. D. Glinchuk, J. A. McLeod, A. Moewes, T. P. Surkova, and N. H. Hong, Phys. Rev. B **85**, 165319 (2012).

[23] V. Golovanov, N. Ozcan, M. Viitala, T. T. Rantala, and J. Vaara, in *Nanodevices and Nanomaterials for Ecological Security*, NATO Science for Peace and Security Series B: Physics and Biophysics (Springer, Dordrecht, 2012), pp. 315–323.

[24] C. Wang, Q. Wu, H. L. Ge, and T. Shang, and J. Z. Jiang, Nanotechnology **23**, 075704 (2012).

[25] C. Kilic and A. Zunger, Phys. Rev. Lett. **88**, 095501 (2002).

[26] C. Das Pemmaraju, and S. Sanvito, Phys. Rev. Lett. **94**, 217205 (2005).

[27] W. Wei, Y. Dai, M. Guo, K. Lai, and B. Huang, J. Appl. Phys. **108**, 093901 (2010).

[28] W. Wei, Y. Dai, M. Guo, Z. Zhang, and B. Huang, J. Solid State Chem. **183**, 3073 (2010).

[29] M. Mehdi, B. Mohagheghi, and M. Shokooh-Saremi, Semicond. Sci. Technol. **19**, 764 (2004).

[30] J. Haines and J. M. Léger, Phys. Rev. B **55**, 11144 (1997); A. A. Bolzan, C. Fong, B. J. Kennedy, and C. J. Howard, Acta Crystallogr. Sect. B **53**, 373 (1997).

[31] P. Hohenberg and W. Kohn, Phys. Rev. **136**, B846 (1964).

[32] J. M. Soler *et al.*, J. Phys. Condens.: Matter **14**, 2745 (2002).

[33] J. P. Perdew and A. Zunger, Phys. Rev. B **23**, 5048 (1981).

[34] D. R. Hamann, M. Schlúter, and C. Chiang, Phys. Rev. Lett. **43**, 1494 (1979).

[35] L. Kleinman and D. M. Bylander, Phys. Rev. Lett. **48**, 1425 (1982).

[36] W. H. Press, B. P. Flannery, S. A. Teukolsky, and W. T. Vetterling, *New Numerical Recipes* (Cambridge University Press, New York, 1986).

[37] I. Nekrasov, M. Korotin, and V. Anisimov, arXiv:cond-mat/0009107v1.

[38] S. G. Park, B. Magyari-Kope, and Y. Nishi, Phys. Rev. B **82**, 115109 (2010).

[39] G. Kresse and J. Furthmuller, Phys. Rev. B, **54**, 11169 (1996).

[40] A. F. Kohan, G. Ceder, D. Morgan, and C. G. deWalle, Phys. Rev. B **61**, 15019 (2000).

[41] K. Yang, Y. Dai, and B. Huang, arXiv:1202.5651v1 [cond-mat].

[42] J. A. Berger, L. Reining, and F. Sottile, Phys. Rev. B **85**, 085126 (2012).

[43] Silva *et al.*, Phys. Scr. T **109** , 180 (2004).

[44] J. A. Dean, ed., *Langes Handbook of Chemistry*, 14th ed. (McGraw-Hill, New York, 1992).

[45] A. Droghetti, C. D. Pemmaraju, and S. Sanvito, Phys. Rev. B **78**, 140404(R) (2008).

[46] V. Fernandes, R. J. O. Mossanek, P. Schio, J. J. Klein, A. J. A. de Oliveira, W. A. Ortiz, N. Mattoso, J. Varalda, W. H. Schreiner, M. Abbate, and D. H. Mosca, Phys. Rev. B **80**, 035202 (2009).

[47] G. Rahman, V. M. García-Suárez, and J. M. Morbec, J. Magn. Magn. Mater. **328**, 104 (2013).

[48] J. M. Morbec and G. Rahman, Phys. Rev. B **87**, 115428 (2013).

[49] M. H. F. Sluiter, Y. Kawazoe, P. Sharma, A. Inoue, A. R. Raju, C. Rout, and U. V. Waghmare, Phys. Rev. Lett. **94**, 187204 (2005).

[50]While revising our manuscript we found that Srivastava *et al.* (arXiv:1302.4869v1 [cond-mat]) have found ferromagnetism in Li-doped SnO_2. Their results confirmed our theoretical work.

[51]C. Zhang and S. Yan, J. Appl. Phys. **106**, 063709 (2009).

[52]H. Wang, Y. Yan, X. Du, X. Liu, K. Li, and H. Jin, J. Appl. Phys. **107**, 103923 (2010).

[53]N. H. Hong, J. Sakai, W. Prellier, and A. Hassini, J. Phys.: Condens. Matter **17**, 1697 (2005).

[54]P. Reunchan, X. Zhou, S. Limpijumnong, A. Janotti, and C. G. V. de Walle, Curr. Appl. Phys. **11**, S296 (2011)

[55]S.-G. Park, B. Magyari-Kópe, and Y. Nishi, Phys. Rev. B **82**, 115109 (2010).

[56]A. Janotti and C. G. Van de Walle, Phys. Status Solidi B **248**, No. 4, 799 (2011).

[57]R. Sanizn, Y. Xu, M. Matsubara, M. N. Amini, H. Dixit, D. Lamoen, and B. Partoens, J. Phys. Chem. Solids **74**, 45 (2013).

[58]A. Janotti, J. B. Varley, P. Rinke, N. Umezawa, G. Kresse, and C. G. Van de Walle, Phys. Rev. B **81**, 085212 (2010).

[59]D. J. Carter, M. Fuchs, and C. Stampf, J. Phys.: Condens. Matter **24**, 255801 (2012).

[60]R. Ramprasad, H. Zhu, P. Rinke, and M. Scheffler, Phys. Rev Lett. **108**, 066404 (2012).

[61]C. D. Pemmaraju, T. Archer, D. Sánchez-Portal, and S. Sanvito, Phys. Rev B **75**, 045101 (2007).

[62]P. Siewak, J. Vanhellemont, and K. J. Kurzydlowski, J. Appl. Phys. **110**, 063534 (2011).